JCTC Journal of Chemical Theory and Computation

Article

pubs.acs.org/JCTC

Surface Adsorption in Nonpolarizable Atomic Models

Jonathan K. Whitmer,[†,‡,¶] Abhijeet A. Joshi,[†] Rebecca J. Carlton,[†] Nicholas L. Abbott,[†] and Juan J. de Pablo*[,¶,§]

[†]Department of Chemical and Biological Engineering, University of Wisconsin, Madison, Wisconsin 53706-1691, United States

[‡]Institute for Molecular Engineering, Argonne National Laboratory, Argonne, Illinois 60439, United States

[¶]Institute for Molecular Engineering, University of Chicago, Chicago, Illinois 60637, United States

[§]Institute for Molecular Engineering, Argonne National Laboratory, Argonne, Illinois 60439, United States

ABSTRACT: Many ionic solutions exhibit species-dependent properties, including surface tension and the salting-out of proteins. These effects may be loosely quantified in terms of the Hofmeister series, first identified in the context of protein solubility. Here, our interest is to develop atomistic models capable of capturing Hofmeister effects rigorously. Importantly, we aim to capture this dependence in computationally cheap "hard" ionic models, which do not exhibit dynamic polarization. To do this, we have performed an investigation detailing the effects of the water model on these properties. Though incredibly important, the role of water models in simulation of ionic solutions and biological systems is essentially unexplored. We quantify this via the ion-dependent surface attraction of the halide series (Cl, Br, I) and, in so doing, determine the relative importance of various hypothesized contributions to ionic surface free energies. Importantly, we demonstrate surface adsorption can result in hard ionic models combined with a thermodynamically accurate representation of the water molecule (TIP4Q). The effect observed in simulations of iodide is commensurate with previous calculations of the surface potential of mean force in rigid molecular dynamics and polarizable density-functional models. Our calculations are direct simulation evidence of the subtle but sensitive role of water thermodynamics in atomistic simulations.

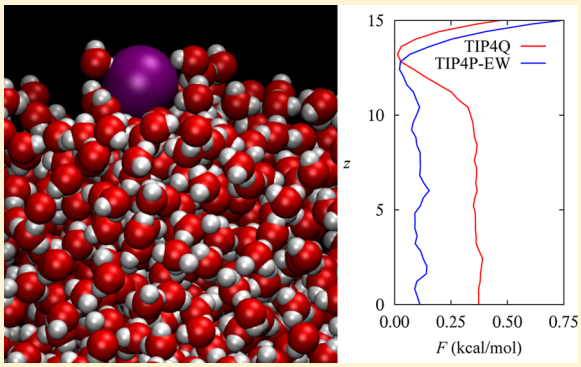

1. INTRODUCTION

The Hofmeister series, and the associated Hofmeister effects, codify ion-specific phenomena which occur in otherwise physically identical systems.[1−5] For even simple monovalent aqueous electrolytes, changing the cationic or anionic species results in nontrivial behavior. Effects include quantifiable changes in surface tension of the electrolyte solution,[6,7] the biologically relevant salting-out (or in) of proteins,[2,8,9] and the ion dependent anchoring aqueous−liquid crystal interfaces.[10,11] This latter situation is particularly interesting for liquid crystal sensing applications,[12,13] where anchoring changes at a planar interface or droplet surface[14,15] engender a morphological transition useful for analyte detection. The ability of dissolved salts to prime a surface for morphological transition enables detection of vanishingly small concentrations of analyte. Much like the variable surface tensions and salting-out effects, anchoring interactions are thought to be influenced by an increased adsorption of ionic species to the hydrophobe−water interface (including optimally hydrophobic water−vapor interfaces), with the resulting local charge imbalance interacting with permanent dipoles on the mesogen. To utilize these phenomena technologically, one must understand the cause of adsorption and the interplay of adsorbed ions with the interface. This is greatly facilitated by the development of atomic models for molecular simulation of the interfacial equilibrium. While our long-term aim is to arrive at a model for liquid crystal−water interfaces with ions, in this investigation we begin by examining the behavior of ions at water−air interfaces for promising nonpolarizable classical models.

While the origin of Hofmeister effects is an old problem, in the context of atomistic models of electrolytes it remains unsolved. Ions have historically been classified as *kosmotropes* or *chaotropes* depending on their perceived influence over local water structure,[2,16] and these classifications overlap well with many observed phenomena. [These names are largely historic and do not pertain to the actual structure-influencing properties of salts, as noted by Zanghi.[16]] Concerning interfacial adsorption, at least six explanations for the Hofmeister series have been presented, which may be identified by what they determine to be the dominant component of the interfacial energy: ion polarization,[17−21] ion solvation,[22,23] ion size,[24,25] interfacial charge and cavitation,[26,27] ionic dispersion forces,[28] and delicate balances between electrostatic and Lennard-Jones (LJ) forces.[29,30] These investigations can all capture a qualitative effect promoting surface adsorption but disagree (often strongly) with each other about the magnitude of adsorption. Importantly, the mechanisms mentioned previously

Received: June 23, 2014
Published: October 21, 2014

   dx.doi.org/10.1021/ct5005406 | *J. Chem. Theory Comput.* 2014, 10, 5616−5624

Table 1. Parameterization of the Four-Site TIP4P,[38] TIP4P-EW,[39] and TIP4Q[40] Models[a]

model	σ (Å)	ε (kJ/mol)	δ (Å)	q_H	q_O	q_M
TIP4P	3.154	0.65020	0.150	0.52	0	−1.04
TIP4P-EW	3.16435	0.68104	0.1250	0.52422	0	−1.04844
TIP4Q	3.16666	0.77491	0.0690	0.525	0.5	−1.55

[a]The geometry of each is similar, with hydrogen atoms a located at a distance 0.9572 Å away from the oxygen atom, forming an angle of 104.52 degrees. A fictive charge site M is located at distance δ from the oxygen atom along the bisector of the HOH angle.

are intimately tied. LJ forces, for example, account for size, averaged dispersion, and induced dipolar forces. The currently prevailing hypothesis ascribes ion adsorption to the polarizability of large, *soft* anions, whose charge can remain highly solvated while the ion itself migrates to the interface to placate the bulk hydrogen bonding network.[20] Importantly, however, the work in refs 7, 22, 29, and 30 has shown that strong polarization is not necessary to obtain surface adsorption—it can be observed with *hard* ion models through alteration of the ionic charge (and thus the electrostatic balance)[29,30] using simple, rigid water models such as SPC/E[31] or the minimalist Stockmayer fluid.[32] Notably, a nonpolarizable force field for iodide[22] and a fully polarizable DFT-based calculation[20] observe similar shallow minima in the potential of mean force (PMF) between an ion and the aqueous interface. Values for the adsorption free energy of iodide are in broad agreement between these models, with the observed minimum ≈0.5 kcal/mol deep in dielectric continuum theory calculations,[24] ≈ 1 kcal/mol deep in density-functional molecular dynamics calculations,[20] ≈ 0.2−0.6 kcal/mol deep in nonpolarizable molecular dynamics simulations,[7,22] ≈ 0.5 kcal/mol in simulations of nonpolar salts with polarizable water,[33] and ≈1.6 kcal/mol and larger for polarizable and partially charged models.[17,18,30,34] Further, ref 29 demonstrated superexponential scaling for surface concentrations of ions as a function of the ionic polarizability, which can overshadow other effects if improperly parametrized.

Note that all simulations involve some level of coarse-graining or approximation in order to facilitate sampling. Increasingly detailed descriptions are met with the simultaneous challenges of accurate parametrization and computational efficiency. First-principles simulations using ab initio DFT-D[20] still fail to replicate the water density, requiring empirical corrections. Coarse-graining into polarizable point-charge models can increase efficiency and improve sampling, but due to the large discrepancies between these surface PMFs and other calculations, the parametrization of the models utilized may be inadequate.[7] Still faster calculations are possible with classical point-charge models and LJ interactions. LJ interactions encompass a myriad terms of polarizable origin into a spherically symmetric potential; a properly parametrized model should be able to capture all of the relevant physics for surface adsorption. As simulations have had success in altering the charge[29,30,35−37] or LJ parameters[22] of point-charge models to describe ionic properties such as protein binding and adsorption, it is relevant to ask if one can simultaneously have an ionic model with the correct bulk properties that also exhibits surface adsorption. Within this work, our intent is to examine whether surface adsorption naturally arises when water model and ion models have each been parametrized to match bulk thermodynamic behavior. We will consider the relative influence of two water models (TIP4P-EW[38,39] and TIP4Q[40]) on a single ionic model. We demonstrate that, owing to close matching between ion solvation and surface potential terms, these two models exhibit nearly identical bulk solvation thermodynamics, with TIP4Q additionally promoting adsorption of iodide ions. Examining the energetic contributions, we find that a primary role in segregation is played by the water−water enthalpy, as suggested by recent work.[17,30,34,41] Though these interactions are not directly responsible for adsorption, it is their contribution to solvation entropy[42] which provides the driving force for segregation. This result is consistent with the results of charge-scaling models[35−37] which adjust ionic charges based on the dielectric constant of water, as TIP4Q has been explicitly designed to match this property, in contrast to TIP4P. In what follows, we will present evidence that the charge distribution of TIP4Q alters the energetics of the ion−water system and leads to adsorption, while retaining near-identical solvation properties to TIP4P.

2. METHODS

The TIP4Q model[40,43] is a modification of the standard TIP4P geometry of water, having a single Lennard-Jones site for the oxygen four sites for electrostatic interactions. Previous investigations[40] have demonstrated close matching between this model and the thermodynamic properties of water over a wide temperature range, in contrast to other rigid point-charge models. In TIP4P, there are four points (oxygen, two hydrogens, and a fictive site M) which hold three partial charges (two positive hydrogens balanced by the M site). TIP4Q adds an additional positive charge onto the oxygen atom. This subtle modification originates from a desire to match the dielectric properties of water by adding an extra degree of freedom (the dipole moment) into a four-site rigid model.[40] The resulting structural properties and equations of state are very similar to that of other TIP4P-based models, thus it should exhibit similar thermodynamic behavior when utilized with (e.g.) biomolecules parametrized for this class. An important second consequence of the four-charge model is its effect on hydrogen bonding. This arrangement is able to limit the strength of hydrogen bonds relative to TIP4P, which allows the extended hydrogen atom to protrude into the ostensibly excluded region surrounding the oxygen atom, an effect which manifests in a closer match in vaporization enthalpies and heat capacities relative to other four-site models.[40] In this work, we will compare the performance of the TIP4Q model to that of the TIP4P-EW.[39]model, a variant of TIP4P altered for better accuracy in periodic geometries using the Ewald sum. The differences between the three models are depicted in Table 1.

We are interested here in three sets of information: the solvation free energy $\Delta G^{full}_{solvation}$ of the ion, the adsorption behavior of simulated salt solutions, and the potential of mean force for ions near an otherwise neat water−vapor interface. The first set of investigations uses standard techniques of thermodynamic integration,[44] along with surface potential,[42] pressure,[45,46] and periodic image corrections[46,47] to compare single-ion solvation energies in simulation to experimental values. Using the validated ions, we examine the behavior of

dx.doi.org/10.1021/ct5005406 | J. Chem. Theory Comput. 2014, 10, 5616−5624

sodium halide salts in aqueous solutions defined by the two models in velocity-Verlet molecular dynamics (MD). Finally, we compute the potential of mean force for model iodide ions near the Gibbs dividing surface (GDS) via umbrella sampling[44] on the ion's position. Thermodynamic integration is partially performed in the NPT ensemble, while all other simulations are performed in the canonical ensemble. Further simulation details follow in the model validation and result discussion sections.

The work in ref 48 demonstrated that ion models are often thermodynamically misparametrized, despite there being only two adjustable parameters (the Lennard-Jones parameters). The proper parameters for ion interactions are sensitive to the water model used as well as the mixing rules for LJ interactions. Ion parameters obtained from standard parametrizations[49−52] have been shown to crystallize at large, unphysical concentrations in simulation,[53−56] meaning their association energy and solvation energy were mismatched. Some simulations avert this problem by utilizing other parametrizations[54,57] without concern for their thermodynamic origin. A central quantity in more careful parametrizations must be the solvation free energy, $\Delta G_{solvation}$, which is computed by thermodynamic integration for the insertion and charging of an ion.[46,48] This proceeds in two steps, each controlled by a parameter λ tuned between 'off' (0) and 'on' (1) states: the insertion of the ion [with associated energy $U_{LJ}(\lambda_{LJ}) = \Sigma_i \lambda_{LJ} \varepsilon_{ij}[(\sigma_{ij}/r_{ij})^{12} - (\sigma_{ij}/r_{ij})^6]$, where i runs over all atoms interacting with the ion (j)], and the charging of the ion [with associated energy $U_{Coulomb}(\lambda_{Coulomb}) = \Sigma_i \lambda_{Coulomb} q_i q_j / r_{ij}$]. To avoid singularities, these interactions are performed sequentially, with a strong soft potential initially wrapping the growing ion.[58,61] One may self-consistently fit the ion parameters through a combination of ion solvation free energy $\Delta G_{solvation}$ and ionic lattice potential energy $U_{lattice}$.[48] Whereas previous parametrizations focused primarily on $\Delta G_{solvation}$, while targeting also the ion−water minimum distances and distribution functions, ref 48 used both $\Delta G_{solvation}$ and $U_{lattice}$ to examine three different models—SPC/E,[31] TIP3P,[38] and TIP4P-EW,[39] finding that simple halides parametrized for each of these models exhibited solvation energies which differ from experimentally reported values[45] of $\Delta G_{solvation}$ by 2% or more, while also having significant deviation from the lattice constants and lattice energy. Thus, the values reported in ref 48 can be considered the best available ionic models for each of the three water models used therein. A similar effort was undertaken in ref 46, focusing on the SPC/E rather than the TIP-derived models considered here. We therefore utilize the ion parameters of ref 48 for our TIP4P-EW comparisons. For completeness, the ion parameters used here as well as the parameters of various other commonly utilized ion models are listed in Table 2. Note that a general feature of these ions versus others in common use with TIP4P-derived models (cf. refs 48−54, 57, and references therein) is that anions tend to be larger, implying increased cavitation, in line with previous observations of adsorption in unphysically large iodide models.[23] Another ion model with these features is that of Horinek et al.,[22,46] which coincidentally are known to exhibit surface adsorption in SPC/E water. The solvation-based parametrization leads to a decreased Lennard-Jones strength ε for ions throughout the halide series, implying weaker binding for these larger ions. Each of these properties addresses a driving force in surface adsorption and may be expected to promote such behavior.

TIP4Q currently has no specific ion parametrizations. However, some work on embedding ions has been performed;

Table 2. Ionic Parameters from Ref 48 Utilized within This Work[a]

species	σ (Å)	ε (kJ/mol)
Na^{+48}	2.185	0.7047
Cl^{-48}	4.918	0.0488
Br^{-48}	4.932	0.1271
I^{-48}	5.260	0.1745
Na^{+52}	4.012	0.0021
Cl^{-52}	3.967	2.9706
Br^{-52}	4.194	2.9706
I^{-52}	4.639	2.9706
Na^{+49}	3.328	0.0116
Cl^{-50}	4.455	0.4184
I^{-51}	5.149	0.4184
Na^{+46}	2.22	1.54
Cl^{-46}	4.52	0.42
Br^{-46}	5.05	0.21
I^{-46}	5.71	0.16

[a]Interaction parameters for the commonly used Åqvist[49]−Dang[50,51] and Jensen−Jorgensen[52] parameterizations are also given. Lorentz-Berthelot[60] combining rules are used to obtain mixed interaction parameters. Note that Br^- was not parameterized by Dang.[50,51] An additional parameterization due to Horinek et al.,[22,46] which exhibits surface adsorption in the SPC/E model, is also given.

utilizing the previously noted ionic model for TIP4P-EW,[48] ref 43 examined the precipitation of saturated solutions of NaCl and NaI. They noted that these systems did not form crystals; this behavior was attributed to a lack of repulsion in cation−M and anion−hydrogen interaction pairs. To restore proper crystal equilibrium, a damping potential was applied to these interactions. Such a potential will necessarily modify the solvation free energy and require a complete refitting of solvation and lattice energies. Note that because of this, one might expect the solvation free energies of model ions within TIP4Q to differ strongly from experimental data. In Figure 1 we plot the solvation energy for halide ions in TIP4Q and

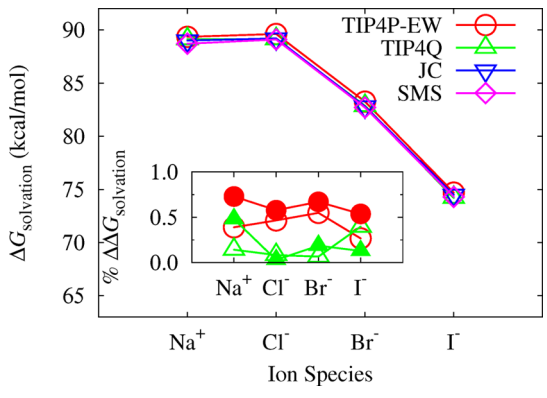

Figure 1. Solvation energy for ions in TIP4P-EW and TIP4Q water measured in this work, compared with the solvation energies for TIP4P-EW calculated by Joung and Cheatham (JC)[48] and the values reported by Schmid, Miah, and Sapunov (SMS).[45] Both the absolute solvation energy and the percent difference ($\Delta\Delta G$) with Joung and Cheatham's work (open symbols) and with experiments (solid symbols) are reported. Solvation energies are matched well without extra parametrization[48] in TIP4Q simulations.

dx.doi.org/10.1021/ct5005406 | J. Chem. Theory Comput. 2014, 10, 5616−5624

TIP4P-EW utilizing the ions of ref 48 and compare them both to the previously reported[48] and experimental values.[45] These calculations were performed using the software package GROMACS[59,61] in the *NPT* ensemble for a single ion in bulk water. N = 1000 water molecules are used in a box of starting dimension $L \times L \times 2.08L$ (L = 27.2 Å). Charge interactions were calculated using the PME algorithm, under which the energy diverges, but forces remain finite. To renormalize the energies, a neutralizing jellium background was assumed, whose energy contributes negligible corrections to the solvation energy within the system. For each of Na^+, Cl^-, Br^-, and I^-, our calculations differ from literature results by less than 0.5% (cf. Figure 1, inset), with particularly good matching between the experimental values in ref 45 and our calculated solvation energies for TIP4Q.

It should be noted that ref 48 ignores some potentially important contributions from surface free energy,[42,46] compression free energy,[46,62] and periodic self-energy.[46,47] A more accurate model may potentially be obtained by adapting this model to fit the experimental values of Tissandier et al.[63] instead. This introduces three further contributions to the solvation energy

$$\Delta G^{\mathrm{full}}_{\mathrm{solvation}} = \Delta G_{\mathrm{solvation}} + N_{\mathrm{A}} z e \phi_{\mathrm{surface}} + N_{\mathrm{A}} k_{\mathrm{B}} T \log(p_1/p_0) + \Delta G_{\mathrm{Ewald}} \quad (1)$$

The first term is due to the electric potential ϕ_{surface} of water−vapor surfaces which must be crossed in order to solvate the ion. The second term (with N_{A} equal to Avogadro's constant) is included in the solvation pathway utilized for experimental energies[45] which details the compression of an ideal gas at p_0 = 1 atm to a pressure of p_1 = 24.6 atm, corresponding to an ideal 1 M solution. The final correction is due to Ewald self-energies and the interactions incurred with periodic images of the solvation cell. Explicit expressions for these corrections are found elsewhere.[46,47,62] Importantly, after subtracting the standard Ewald contribution from a charged cell (due to neutralization of the ion by a uniform jellium background), the remaining corrections detailed in ref 46 are negligible (<1 kcal/mol) relative to surface potential and compression contributions to the free energy.

It can be verified that surface-potential effects for the two water models are nearly identical through molecular dynamics simulations of neat water−vapor interfaces.[64] These simulations are performed by monitoring an $L \times L \times L$ slab of water in a $L \times L \times 2L$ simulation box (L = 31.06 Å). Our simulations with TIP4P-EW and TIP4Q demonstrate near-identical surface potentials (each ≈0.52 V), plotted in Figure 2. Combining this effect [± 12.0 kcal/mol for anions (+) and cations (−), respectively] and the compression free energy (≈1.9 kcal/mol) results in $\Delta G^{\mathrm{full}}_{\mathrm{solvation}}$ for halides which achieve near agreement with the hydration free energies of Tissandier.[46,63]

Some discrepancy still exists. Starting with the solvation energies reported by Schmid,[45] addition of the pressure correction leaves a shift $\Delta G^{\mathrm{full}}_{\mathrm{solvation}} = \pm 14.5$ kcal/mol for anions and cations, respectively, implying a surface potential of ≈−0.63 V. Hence, a water model which correctly represents this surface potential value should be able to identically match both refs 63 and 45 using the appropriate thermodynamic terms. As our surface potentials do not identically match this, the values in Figure 1 suffice for comparison. [This is true for all of the common point-charge models for water. SPC/E has a surface potential of −13.8 kcal/mol-e[27,42,65] or −0.598 V. This value is closer to the −14.5 obtained by comparing Tissandier et al. results[63] to Schmid et al.,[45] though this does not correspond to the true surface potential for water, as is discussed in detail elsewhere.[42]]

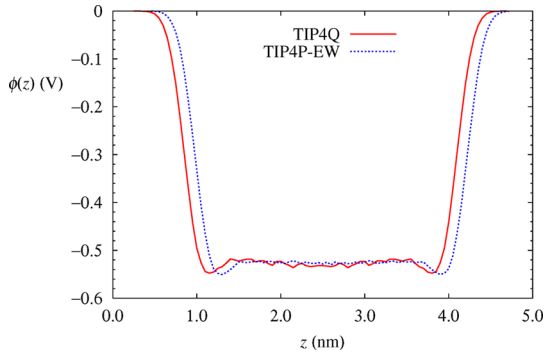

Figure 2. Surface potential $\phi(z)$ for TIP4P and TIP4Q water models measured in molecular dynamics simulation. Both models give a value $\phi_{\mathrm{surface}} \approx -0.52$ V. The plots are slightly offset in z and have been symmetrized about the slab center for clarity.

Additionally, by simulating a crystal in equilibrium with TIP4Q solvent at 353 K, we may demonstrate stabilization in the size of crystals as a function of time. The temperature of these simulations was chosen in order to maximize ionic diffusion, so that any growth or dissolution of the crystal phase will occur on easily accessible time scales. To determine the simulation molality, the largest cluster size in simulation (defining the crystal in equilibrium with the solute) is monitored. Clusters are computed by inclusion of all ions within the interatomic distance for the simulated crystal.[48] Here we performed 20 ns runs in contact with crystalline NaI, beginning at 15 mol/kg of solute which decreases slightly to 14 mol/kg over the course of a run. Our simulations slightly overestimate crystal stability relative to experimental conditions,[66] likely due to finite size effects and periodic boundary conditions, but demonstrate convincingly the presence of solute−crystal equilibrium with no modifications necessary to the water−ion potential, in contrast to ref 43, which found that crystals failed to nucleate without such modifications (though, importantly, such behavior involves nucleation barriers within the system rather than solvent−solute equilibrium alone). Further, it should be noted that at such high concentrations, many-body effects contribute to ionic interactions[67] and thus ostensibly affect the ion−water solvation equilibrium if unaccounted for.

Noting that we now have a common ionic model which exhibits correct solvation thermodynamics in two different water models, we proceed to study the solvation behavior of simple halide ions.

3. RESULTS AND DISCUSSION

Having established the solvent−solute thermodynamics, we proceed to investigate surface adsorption. Using the model outlined above, we have performed molecular dynamics simulations of ten NaX pairs (where X = Cl, Br, I) within a solvent consisting of 844 water molecules. *NVT* conditions are utilized, with box dimensions $L \times L \times 2.91L$ (L = 37.3 Å) at temperature T = 298 K with periodic boundaries. The water is arranged such that periodic images of the water are separated by a vapor (air) layer. This simple simulation leads to intriguing results. We plot in Figure 3 a comparison between the surface-

dx.doi.org/10.1021/ct5005406 | J. Chem. Theory Comput. 2014, 10, 5616−5624

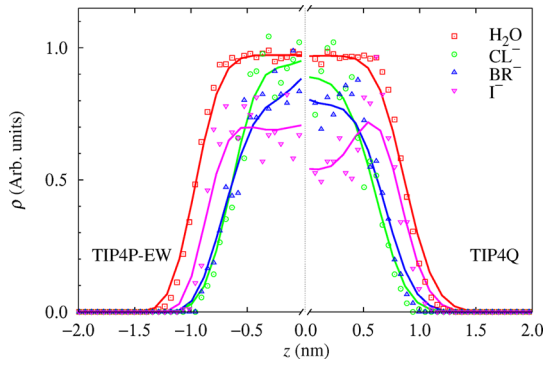

Figure 3. Relative adsorption of halide series ions in TIP4P-EW (left) and TIP4Q (right). While all ions in TIP4Q experience a slightly enhanced probability for the interfacial region relative to TIP4P-EW, iodide experiences a clear tendency to adsorb not present in the TIP4P-EW model. The water density is given in terms of (g/cm^3), while ion densities are given in g/cm^3 divided by their molar mass so they may be plotted on the same scale.

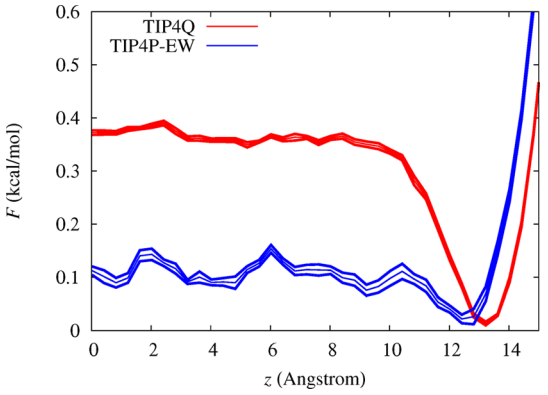

Figure 4. Adsorption energy of the iodide ion to the water−air interface calculated using umbrella sampling for a single ion embedded in solvent. Note that iodide in both models a net attraction to the interface, which is enhanced in TIP4Q. The depth of the local interaction, 0.4 kcal/mol is $\approx 0.6 k_B T$. The three bunched curves refer to the mean Helmholtz energy, and its upper and lower error bars are computed via bootstrap methods.[68]

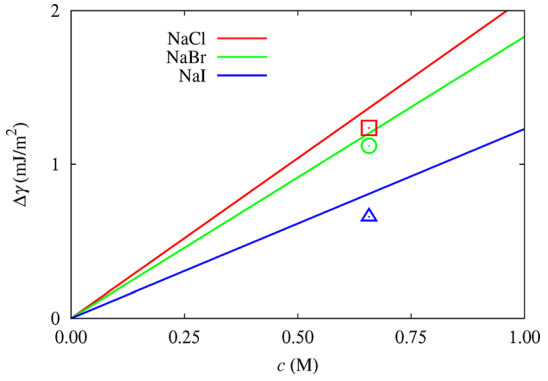

Figure 5. Estimated surface tensions calculated from molecular simulations of Figure 3 using TIP4Q. Lines are for the mean value of $d(\Delta\gamma)/dc$ in the experimental data of ref 71, while symbols are from simulation data using the integral approximation $\Delta\gamma = -k_B T \sum_i \Gamma_i$, with index i running over the ionic species, and Γ_i being the surface excess of species i. While exact agreement is not achieved, the order of magnitude and trend of the halides is observed.

adsorptive behavior of TIP4P-EW and TIP4Q for these halides. As expected for hard ion simulations, there is no adsorption of chloride ions for either water model. In contrast, iodide is seen to strongly adsorb at the interface of TIP4Q water, with the probability of particles being found within a slab of width Δz at the surface approximately 5/3 that of the same ion being found in the bulk. This contrasts with the lack of significant adsorption in TIP4P-EW. While similar results have previously been reported for hard ion models which match ion−water characteristics for a fixed water model,[22] our observation is significant in that the results in this model are a direct consequence of matching the ionic solvation free energy and the thermodynamics of water. [It should be mentioned that this work is also able to capture semiquantitatively the trends in surface tension observed in experiment.] Importantly, the dielectric constant of TIP4Q matches the experimental value for liquid water, while it is underestimated by TIP4P-EW; this offers a potential connection to the charge-scaling theory in ref 37.

To probe this effect in greater detail, we also performed simulations of a single iodide ion embedded in a water slab. N = 1000 water molecules were used, within a box of geometry $L \times L \times 2L$ (L = 30.06 Å). After an equilibration period, the iodide ion was inserted into the water slab at a desired depth. We then performed umbrella sampling simulations[44] to probe the free energy of the system as a function of the ion separation from the slab center of mass and reconstructed the free energy using multiple-histogram reweighing.[68,69] The results are plotted in Figure 4. For both water models, a minimum is observed in the free energy at $z \approx 13$ Å. This minimum is deeper for the TIP4Q model and shifted toward the Gibbs dividing surface (GDS). Importantly, both models remain explicitly solvated, with the minimum free energy $\gtrsim \sigma/2$ away from the GDS, in agreement with the nonpolarizable simulations of ref 22 but in contrast to partial-charge models models.[30] Note that the character of the adsorption seen here is important, in that the Gibbs adsorption isotherm gives a net tendency for particles to localize at the surface over the bulk. Such weak adsorption *near* the GDS, with depletion of both ion types from the GDS, should have the effect of raising the surface tension as ionic strength is increased, consistent with experiments.[2] Weakly adsorbing species such as the iodide, along with enhanced interactions between oppositely charged ions near the vapor interface,[70] will then partially negate this increase in surface tension. A back-of-the envelope calculation utilizing the ionic profiles computed in Figure 3 confirms this observation (cf. Figure 5) and shows order of magnitude agreement between our simulations and experimental measurements of this surface tension.[71]

It is instructive to examine the energetic effects leading to this adsorption. Following the work of ref 30, we plot the energy contributions from water−water and water−ion interactions in Figure 6 as a function of distance from the aqueous interface, using data from umbrella calculations. These calculations were performed for water in a slab geometry using the LAMMPS simulation package with P3M electrostatics.[72] We impose the interface through restriction of the water molecules to a subset of the box. We further limit the motion of the ion by imposing harmonic umbrellas on its position normal to the water−air interface. We find that, as was previously reported,[30,41] the adsorption interaction between the iodide ion and the interface is affected by bulk energetics. This is evidenced by the enhanced solvent−solvent interaction energies apparent in Figures 6 (a−d). The energetic differences

dx.doi.org/10.1021/ct5005406 | J. Chem. Theory Comput. 2014, 10, 5616−5624

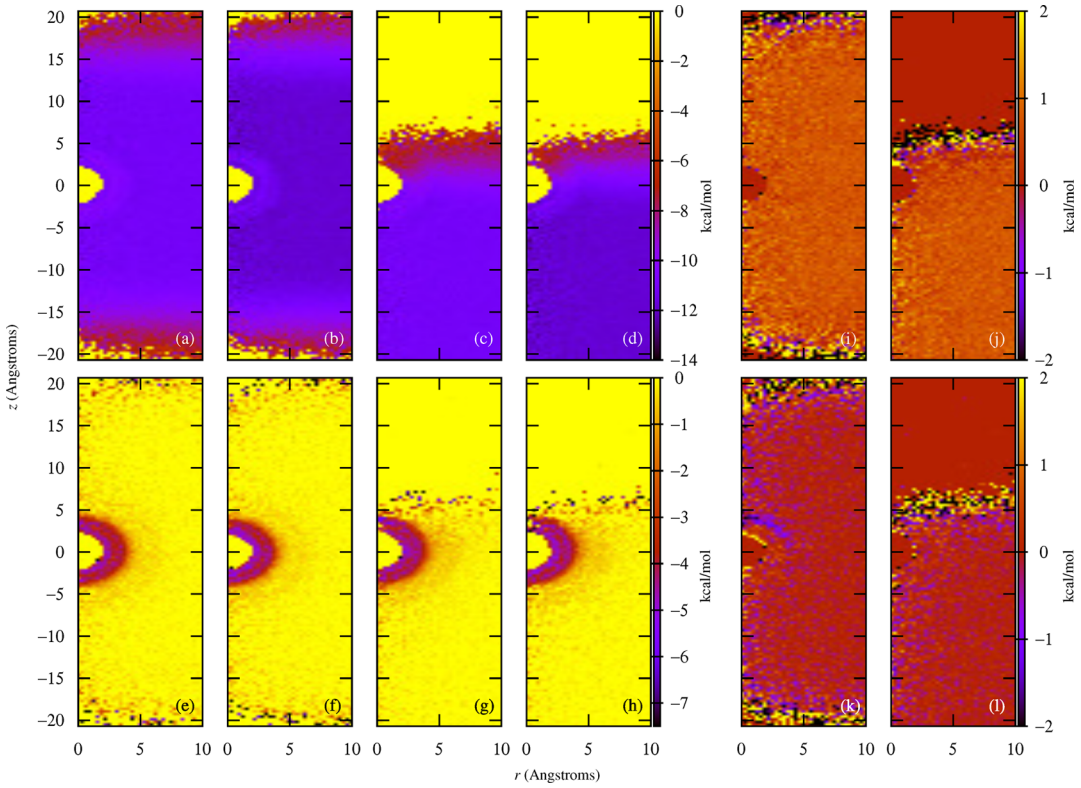

Figure 6. Spatial decomposition of the solvent−solvent and solvent−ion binding energies for an ion in TIP4P-EW (left of each pair) and TIP4Q (right of each pair) water. (a−d) Solvent−solvent contributions to the energy for (a,b) an ion positioned in bulk water or (c,d) an iodide ion positioned at z = 15 Å, near the Gibbs dividing surface (and the minimum of the free energy in Figure 4). (e,f) Ion−solvent contributions to the energy for the analogs of (a) and (b). (g,h) Ion−solvent contributions for the analogs of (c) and (d). Importantly, the bulk solvent−solvent interactions are weakly more favorable for TIP4Q, implying that adsorption within this model is driven by bulk water association. The well-defined hydration shells, visible in the solvent−ion energy maps for TIP4Q, support the claim that the ion significantly disrupts local water structure from the solute-free case. Significant differences in energy distribution (plotted as $U_{\mathrm{TIP4P\text{-}EW}} - U_{\mathrm{TIP4Q}}$) are visible in the solvent−solvent interactions (i,j) and in the solvent−ion interactions (k,l), where TIP4P-EW waters within the hydration shell are seen to bind more strongly to the ion. This is strongly suggestive that both solvent−solvent association and de-emphasized solvent−ion binding drive the adsorption present in TIP4Q.

between bulk water in the TIP4P-EW [Figures 6(a,c)] and TIP4Q [Figures 6(b,d)] models apparently imply that stronger binding for water−water interactions in TIP4Q drives the ion away from the bulk. Importantly, the iodide engenders a significant hydration shell structure that is penalized in both models [cf. Figures 6 (e−h)]. Further, one can easily discern from maps of the energy difference between the two models [Figures 6(i−k)] that all energetic differences arise from solvent−solvent interactions and is suggestive of their role in driving ions to the interface. Within our simulations, the total water−water energy is largely unchanged as the ion moves toward the interface, thus the effect of favorable solvent−solvent interactions is not to directly drive the interaction but to facilitate entropic gain through more readily broken water−water bonds near the interface. Additionally, a small effect is visible in solvent−ion association, where the solvation shell apparent in Figures 6(e−h) disappears upon the ion approaching the interface. This energetic loss for TIP4P-EW solvated ions relative to TIP4Q solvated ions will also act to enhance adsorption in the TIP4Q model. Due to the full thermodynamic properties of TIP4Q being fit to match those of experiments on bulk water, adsorption arises naturally from the thermodynamically accurate model. This result has important implications for interfacial interactions in all-atom simulations, since incorrect water thermodynamics are seen to significantly affect not just quantitative results but the qualitative result of ion adsorption.

4. CONCLUSIONS

In conclusion, we have demonstrated that fully charged, nonpolarizable ions may experience adsorption to the air−water interface as a direct consequence of parametrization of both water and ions which focuses on capturing the bulk thermodynamic and structural behavior of water (through the TIP4Q model[40]) and the bulk solvation equilibrium of ions.[48] In contrast to previous work on the subject which examined the effects of changing ion parameters using a fixed water model,[7,22] here we explicitly demonstrate the subtle, but significant, effects which arise when the water model is varied. Importantly, the surface-adsorption potential within this work is approximately 0.4 kcal/mol in depth, in good agreement both with recent DFT-MD calculations,[20] previous hard ion models optimized for solvation entropy.[22] These results are significant in that they demonstrate that behaviors thought to be a direct result of ion polarizability[18] arise naturally in its absence when the model has been properly thermodynamically parametrized. Importantly, we have identified three effects which promote adsorption in TIP4Q relative to TIP4P-EW: (1) matching of the dielectric constant (which has an effect similar to reducing the effective ionic charge), (2) enhanced solvent−solvent association emphasizing entropic gains at the water−vapor interface for

dx.doi.org/10.1021/ct5005406 | J. Chem. Theory Comput. 2014, 10, 5616−5624

the I^- ion, and (3) weaker solvent−ion binding. While here we have examined only simple ion−water systems, we anticipate that using a model such as TIP4Q will have profound effects on the behavior of molecular ions having non-negligible static multipole moments.[73] Further, the implications for salt-specific protein interactions outlined in the Introduction are obvious, as costly polarization interactions with proteins and lipids[9,57] need not be calculated. However, one must keep in mind that all MD simulations, even atomistic ones, are coarse-grained to some extent. We caution that in more complex systems, solute interactions may need to be adjusted to work with the water model of interest. Of the many currently available molecular force fields (see refs 74 and 75 for recent surveys of various force fields and their accuracy), none has been explicitly parametrized to work with TIP4Q. Given our observations, models parametrized for TIP4P and derived models should nevertheless provide a close approximation to ideal parameters. Note also that additional improvements may still be made to the models in this paper. Our investigations found that the crystal equilibrium of water and NaI is incorrect for stock TIP4Q and ions. Such behavior highlights the complexity in determining mixed Lennard-Jones interactions for water and ions. Appropriately incorporating these interactions will enable accurate simulations of ionic effects in atomistic simulations. Consistent models of ion−water interactions are a necessary first step to creating accurate, standardized atomistic simulation models.

AUTHOR INFORMATION

Corresponding Author

*E-mail: depablo@uchicago.edu.

Notes

The authors declare no competing financial interest.

ACKNOWLEDGMENTS

This work was supported by the University of Wisconsin Materials Research Science and Engineering Center (UW-MRSEC) under National Science Foundation Grant No. DMR-1121288. J.K.W. was partially supported by a NHGRI training grant to the Genomic Sciences Training Program, T32HG002760. The authors acknowledge the use of computational resources accessible through the University of Wisconsin Center for High Throughput Computing, the University of Chicago Midway cluster, and Blues, a high-performance computing cluster operated by the Laboratory Computing Resource Center at Argonne National Laboratory. Development of algorithms and codes employed for this work is supported by the Department of Energy, Basic Energy Sciences, Materials Research Division.

REFERENCES

(1) Cacace, M. G.; Landau, E. M.; Ramsden, J. J. The Hofmeister series: salt and solvent effects on interfacial phenomena. *Q. Rev. Biophys.* **1997**, *30*, 241−277.

(2) Collins, K. D.; Washabaugh, M. W. The Hofmeister effect and the behaviour of water at interfaces. *Q. Rev. Biophys.* **1985**, *18*, 323−422.

(3) Lo Nostro, P.; Ninham, B. W. Hofmeister phenomena: an update on ion specificity in biology. *Chem. Rev. (Washington, DC, U. S.)* **2012**, *112*, 2286−2322.

(4) Zhang, Y.; Cremer, P. S. Chemistry of Hofmeister anions and osmolytes. *Annu. Rev. Phys. Chem.* **2010**, *61*, 63−83.

(5) Kunz, W.; Henle, J.; Ninham, B. 'Zur Lehre von der Wirkung der Salze' (about the science of the effect of salts): Franz Hofmeister's historical papers. *Curr. Opin. Colloid Interface Sci.* **2004**, *9*, 19−37.

(6) Cheng, J.; Vecitis, C. D.; Hoffmann, M. R.; Colussi, A. J. Experimental anion affinities for the air/water interface. *J. Phys. Chem. B* **2006**, *110*, 25598−25602.

(7) Netz, R. R.; Horinek, D. Progress in modeling of ion effects at the vapor/water interface. *Annu. Rev. Phys. Chem.* **2012**, *63*, 401−418.

(8) Zhang, Y.; Cremer, P. S. Interactions between macromolecules and ions: The Hofmeister series. *Curr. Opin. Chem. Biol.* **2006**, *10*, 658−663.

(9) Heyda, J.; Hrobárik, T.; Jungwirth, P. Ion-specific interactions between halides and basic amino acids in water. *J. Phys. Chem. A* **2009**, *113*, 1969−1975.

(10) Carlton, R. J.; Ma, C. D.; Gupta, J. K.; Abbott, N. L. Influence of specific anions on the orientational ordering of thermotropic liquid crystals at aqueous interfaces. *Langmuir* **2012**, *28*, 12796−12805.

(11) Carlton, R. J.; Gupta, J. K.; Swift, C. L.; Abbott, N. L. Influence of simple electrolytes on the orientational ordering of thermotropic liquid crystals at aqueous interfaces. *Langmuir* **2012**, *28*, 31−36.

(12) Lin, I.-H.; Miller, D. S.; Bertics, P. J.; Murphy, C. J.; de Pablo, J. J.; Abbott, N. L. Endotoxin-induced structural transformations in liquid crystalline droplets. *Science* **2011**, *332*, 1297−1300.

(13) Bera, T.; Fang, J. Polyelectrolyte-coated liquid crystal droplets for detecting charged macromolecules. *J. Mater. Chem.* **2012**, *22*, 6807−6812.

(14) Miller, D. S.; Abbott, N. L. Influence of droplet size, pH and ionic strength on endotoxin-triggered ordering transitions in liquid crystalline droplets. *Soft Matter* **2013**, *9*, 374−382.

(15) Tomar, V.; Hernández, S. I.; Abbott, N. L.; Hernández-Ortiz, J. P.; de Pablo, J. J. Morphological transitions in liquid crystal nanodroplets. *Soft Matter* **2012**, *8*, 8679−8689.

(16) Zangi, R. Can salting-in/salting-out ions be classified as chaotropes/kosmotropes? *J. Phys. Chem. B* **2010**, *114*, 643−650.

(17) Caleman, C.; Hub, J. S.; van Maaren, P. J.; van der Spoel, D. Atomistic simulation of ion solvation in water explains surface preference of halides. *Proc. Natl. Acad. Sci. (U. S. A.)* **2011**, *108*, 6838−6842.

(18) Jungwirth, P.; Tobias, D. J. Specific Ion Effects at the Air/Water Interface. *Chem. Rev. (Washington, DC, U. S.)* **2006**, *106*, 1259−1281.

(19) Jungwirth, P.; Winter, B. Ions at aqueous interfaces: from water surface to hydrated proteins. *Annu. Rev. Phys. Chem.* **2008**, *59*, 343−366.

(20) Baer, M. D.; Mundy, C. J. Toward an understanding of the specific ion effect using density functional theory. *J. Phys. Chem. Lett.* **2011**, *2*, 1088−1093.

(21) Archontis, G.; Leontidis, E. Dissecting the stabilization of iodide at the air−water interface into components: A free energy analysis. *Chem. Phys. Lett.* **2006**, *420*, 199−203.

(22) Horinek, D.; Herz, A.; Vrbka, L.; Sedlmeier, F.; Mamatkulov, S. I.; Netz, R. R. Specific ion adsorption at the air/water interface: The role of hydrophobic solvation. *Chem. Phys. Lett.* **2009**, *479*, 173−183.

(23) Huang, D. M.; Cottin-Bizonne, C.; Ybert, C.; Bocquet, L. Aqueous electrolytes near hydrophobic surfaces: dynamic effects of ion specificity and hydrodynamic slip. *Langmuir* **2008**, *24*, 1442−1450.

(24) Levin, Y.; dos Santos, A. P.; Diehl, A. Ions at the air−water interface: An end to a hundred-year-old mystery? *Phys. Rev. Lett.* **2009**, *103*, 257802.

(25) dos Santos, A. P.; Levin, Y. Ions at the water-oil interface: Interfacial tension of electrolyte solutions. *Langmuir* **2012**, *28*, 1304−1308.

(26) Baer, M. D.; Stern, A. C.; Levin, Y.; Tobias, D. J.; Mundy, C. J. Electrochemical surface potential due to classical point charge models drives anion adsorption to the air−water interface. *J. Phys. Chem. Lett.* **2012**, *3*, 1565−1570.

(27) Arslanargin, A.; Beck, T. L. Free energy partitioning analysis of the driving forces that determine ion density profiles near the water liquid-vapor interface. *J. Chem. Phys.* **2012**, *136*, 104503.

(28) Boström, M.; Ninham, B. W. Dispersion self-free energies and interaction free energies of finite-sized ions in salt solutions. *Langmuir* **2004**, *20*, 7569−7574.
(29) Noah-Vanhoucke, J.; Geissler, P. L. On the fluctuations that drive small ions toward, and away from, interfaces between polar liquids and their vapors. *Proc. Natl. Acad. Sci. (U. S. A.)* **2009**, *106*, 15125−15130.
(30) Otten, D. E.; Shaffer, P. R.; Geissler, P. L.; Saykally, R. J. Elucidating the mechanism of selective ion adsorption to the liquid water surface. *Proc. Natl. Acad. Sci. (U. S. A.)* **2012**, *109*, 701−705.
(31) Berendsen, H. J. C.; Grigera, J. R.; Straatsma, T. P. The missing term in effective pair potentials. *J. Phys. Chem.* **1987**, *91*, 6269−6271.
(32) Stockmayer, W. H. Second virial coefficients of polar gases. *J. Chem. Phys.* **1941**, *9*, 398−402.
(33) Ou, S.; Patel, S. Temperature dependence and energetics of single ions at the aqueous liquid-vapor interface. *J. Phys. Chem. B* **2013**, *117*, 6512−6523.
(34) Stern, A. C.; Baer, M. D.; Mundy, C. J.; Tobias, D. J. Thermodynamics of iodide adsorption at the instantaneous air-water interface. *J. Chem. Phys.* **2013**, *138*, 114709.
(35) Vazdar, M.; Pluhařová, E.; Mason, P. E.; Vácha, R.; Jungwirth, P. Ions at hydrophobic aqueous interfaces: Molecular dynamics with effective polarization. *J. Phys. Chem. Lett.* **2012**, *3*, 2087−2091.
(36) Leontyev, I. V.; Stuchebrukhov, A. A. Electronic continuum model for molecular dynamics simulations. *J. Chem. Phys.* **2009**, *130*, 085102.
(37) Leontyev, I.; Stuchebrukhov, A. Accounting for electronic polarization in non-polarizable force fields. *Phys. Chem. Chem. Phys.* **2011**, *13*, 2613−2626.
(38) Jorgensen, W. L.; Chandrasekhar, J.; Madura, J. D.; Impey, R. W.; Klein, M. L. Comparison of simple potential functions for simulating liquid water. *J. Chem. Phys.* **1983**, *79*, 926−935.
(39) Horn, H. W.; Swope, W. C.; Pitera, J. W.; Madura, J. D.; Dick, T. J.; Hura, G. L.; Head-Gordon, T. Development of an improved four-site water model for biomolecular simulations: TIP4P-EW. *J. Chem. Phys.* **2004**, *120*, 9665−9678.
(40) Alejandre, J.; Chapela, G. A.; Saint-Martin, H.; Mendoza, N. A non-polarizable model of water that yields the dielectric constant and the density anomalies of the liquid: TIP4Q. *Phys. Chem. Chem. Phys.* **2011**, *13*, 19728−19740.
(41) Vaikuntanathan, S.; Shaffer, P. R.; Geissler, P. L. Adsorption of solutes at liquid−vapor interfaces: insights from lattice gas models. *Faraday Discuss.* **2013**, *160*, 63−74.
(42) Beck, T. L. The influence of water interfacial potentials on ion hydration in bulk water and near interfaces. *Chem. Phys. Lett.* **2013**, *561*−*562*, 1−13.
(43) Mendoza, F. N.; Alejandre, J. The role of ion−water interactions in the solubility of ionic solutions. *J. Mol. Liq.* **2012**, *185*, 50−55.
(44) Frenkel, D.; Smit, B. *Understanding Molecular Simulation*, 2nd ed.; Academic Press: San Diego, CA, 2002.
(45) Schmid, R. E.; Miah, A. M.; Sapunov, V. N. A new table of the thermodynamic quantities of ionic hydration: values and some applications (enthalpy−entropy compensation and Born radii). *Phys. Chem. Chem. Phys.* **2000**, *2*, 97−102.
(46) Horinek, D.; Mamatkulov, S. I.; Netz, R. R. Rational design of ion force fields based on thermodynamic solvation properties. *J. Chem. Phys.* **2009**, *130*, 124507.
(47) Beck, T. L.; Paulaitis, M. E.; Pratt, L. R. *The Potential Distribution Theorem and Models of Molecular Solutions*; Cambridge University Press: Cambridge, U.K., 2006.
(48) Joung, I. S.; Cheatham, T. E. Determination of alkali and halide monovalent ion parameters for use in explicitly solvated biomolecular simulations. *J. Phys. Chem. B* **2008**, *112*, 9020−9041.
(49) Aaqvist, J. Ion−water interaction potentials derived from free energy perturbation simulations. *J. Phys. Chem.* **1990**, *94*, 8021−8024.
(50) Dang, L. X.; Smith, D. E. Molecular dynamics simulations of aqueous ionic clusters using polarizable water. *J. Chem. Phys.* **1993**, *99*, 6950−6957.
(51) Dang, L. X.; Garrett, B. C. Photoelectron spectra of the hydrated iodine anion from molecular dynamics simulations. *J. Chem. Phys.* **1993**, *99*, 2972−2977.
(52) Jensen, K. P.; Jorgensen, W. L. Halide, ammonium, and alkali metal ion parameters for modeling aqueous solutions. *J. Chem. Theory Comput.* **2006**, *2*, 1499−1509.
(53) Vaiana, A. C.; Westhof, E.; Auffinger, P. A molecular dynamics simulation study of an aminoglycoside/A-site RNA complex: conformational and hydration patterns. *Biochimie* **2006**, *88*, 1061−1073.
(54) Auffinger, P.; Cheatham, T. E.; Vaiana, A. C. Spontaneous formation of KCl aggregates in biomolecular simulations: A force field issue? *J. Chem. Theory Comput.* **2007**, *3*, 1851−1859.
(55) Chen, A. A.; Pappu, R. V. Parameters of monovalent ions in the AMBER-99 forcefield: assessment of inaccuracies and proposed improvements. *J. Phys. Chem. B* **2007**, *111*, 11884−11887.
(56) Savelyev, A.; Papoian, G. A. Inter-DNA electrostatics from explicit solvent molecular dynamics simulations. *J. Am. Chem. Soc.* **2007**, *129*, 6060−6061.
(57) Vácha, R.; Siu, S. W. I.; Petrov, M.; Böckmann, R. A.; Barucha-Kraszewska, J.; Jurkiewicz, P.; Hof, M.; Berkowitz, M. L.; Jungwirth, P. Effects of alkali cations and halide anions on the DOPC lipid membrane. *J. Phys. Chem. A* **2009**, *113*, 7235−7243.
(58) Beutler, T. C.; Mark, A. E.; van Schaik, R. C.; Gerber, P. R.; van Gunsteren, W. F. Avoiding singularities and numerical instabilities in free energy calculations based on molecular simulations. *Chem. Phys. Lett.* **1994**, *222*, 529−539.
(59) *GROMACS*, version 4.5.5; Hess, B.; Lindahl, E.; van der Spoel, D. et al. Published Online, 2011. http://www.gromacs.org/Downloads (accessed Sept 10, 2014).
(60) Allen, M. P.; Tildesley, D. J. *Computer simulation of liquids*; Oxford University Press: Oxford, 1987.
(61) Hess, B.; Kutzner, C.; van der Spoel, D.; Lindahl, E. GROMACS 4: Algorithms for highly efficient, load-balanced, and scalable molecular simulation. *J. Chem. Theory Comput.* **2008**, *4*, 435−447.
(62) Hummer, G.; Pratt, L. R.; Garca, A. E. Free energy of ionic hydration. *J. Phys. Chem.* **1996**, *100*, 1206−1215.
(63) Tissandier, M. D.; Cowen, K. A.; Feng, W. Y.; Gundlach, E.; Cohen, M. H.; Earhart, A. D.; Coe, J. V.; Tuttle, T. R. The proton's absolute aqueous enthalpy and Gibbs free energy of solvation from cluster-ion solvation data. *J. Phys. Chem. A* **1998**, *102*, 7787−7794.
(64) Harder, E.; Roux, B. On the origin of the electrostatic potential difference at a liquid−vacuum interface. *J. Chem. Phys.* **2008**, *129*, 234706.
(65) Shi, Y.; Beck, T. L. Length scales and interfacial potentials in ion hydration. *J. Chem. Phys.* **2013**, *139*, 044504.
(66) *CRC Handbook of Chemistry and Physics*, 93rd ed.; Haynes, W. M., Ed.; CRC Press/Taylor and Francis: Boca Raton, FL, 2012.
(67) Kalcher, I.; Dzubiella, J. Structure-thermodynamics relation of electrolyte solutions. *J. Chem. Phys.* **2009**, *130*, 134507.
(68) Grossfield, A. *WHAM: The Weighted Histogram Analysis Method*, version 2.0.9; University of Rochester: Rochester, NY, 2012. http://membrane.urmc.rochester.edu/content/wham (accessed Sept 20, 2014).
(69) Kumar, S.; Rosenberg, J. M.; Bouzida, D.; Swendsen, R. H.; Kollman, P. A. The weighted histogram analysis method for free-energy calculations on biomolecules. I. The method. *J. Comput. Chem.* **1992**, *13*, 1011−1021.
(70) Venkateshwaran, V.; Vembanur, S.; Garde, S. Water-mediated ion-ion interactions are enhanced at the water vapor-liquid interface. *Proc. Natl. Acad. Sci. (U. S. A.)* **2014**, *111*, 8729−8734.
(71) Weissenborn, P. K.; Pugh, R. J. Surface tension of aqueous solutions of electrolytes: Relationship with ion hydration, oxygen solubility, and bubble coalescence. *J. Colloid Interface Sci.* **1996**, *184*, 550−563.
(72) Plimpton, S. Fast parallel algorithms for short-range molecular dynamics. *J. Comput. Phys.* **1995**, *117*, 1−19.

(73) Baer, M. D.; Mundy, C. J. An ab initio approach to understanding the specific ion effect. *Faraday Discuss.* **2013**, *160*, 89−101.
(74) Beauchamp, K. A.; Lin, Y.-S.; Das, R.; Pande, V. S. Are protein force fields getting better? A systematic benchmark on 524 diverse NMR measurements. *J. Chem. Theory Comput.* **2012**, *8*, 1409−1414.
(75) Lindorff-Larsen, K.; Maragakis, P.; Piana, S.; Eastwood, M. P.; Dror, R. O.; Shaw, D. E. Systematic validation of protein force fields against experimental data. *PloS One* **2012**, *7*, e32131.